Cosmic Masers - from OH to H_0
Proceedings IAU Symposium No. 287, 2012
R.S. Booth, E.M.L. Humphreys & W.H.T. Vlemmings, eds.

doi:10.1017/S1743921312007594

Early results from a diagnostic 1.3 cm survey of massive young protostars

Crystal L. Brogan[1], Todd R. Hunter[1], Claudia J. Cyganowski[2], Remy Indebetouw[1,3], Rachel Friesen[1] and Claire Chandler[4]

[1]National Radio Astronomy Observatory (NRAO),
520 Edgemont Rd, Charlottesville, VA 22903, USA
email: cbrogan@nrao.edu

[2]Harvard-Smithsonian Center for Astrophysics
60 Garden St., Cambridge, MA 02138, USA
[3]University of Virginia, Charlottesville, VA 22903, USA
[4]National Radio Astronomy Observatory (NRAO), Socorro, New Mexico, 87801, 8USA

Abstract. We have used the recently-upgraded Karl G. Jansky Very Large Array (JVLA) to conduct a K-band ($\sim$ 24 GHz) study of 22 massive young stellar objects in 1.3 cm continuum and a comprehensive set of diagnostic lines. This survey is unique in that it samples a wide range of massive star formation signposts *simultaneously* for the first time. In this proceeding we present preliminary results for the 11 sources in the 2-4 kpc distance bin. We detect compact NH_3 cores in all of the fields, with many showing emission up through the (6,6) transition. Maser emission in the 25 GHz CH_3OH ladder is present in 7 of 11 sources. We also detect non-thermal emission in the NH_3 (3,3) transition in 7 of 11 sources.

Keywords. masers, stars: formation, ISM: jets and outflows, ISM: molecules, radio lines: ISM, radio continuum: ISM, infrared: ISM, submillimeter

1. Introduction

The formation of massive stars remains a poorly-understood phenomenon, primarily because they typically form in complex clusters, at distances of several kiloparsecs (see review by Zinnecker & Yorke (2007). Indeed, the tools traditionally used to classify low mass YSOs (primarily near-IR imaging) are largely inapplicable due to extreme dust obscuration, making it a challenge to gauge the evolutionary state of massive young stellar objects (MYSOs). Useful samples of MYSOs have been compiled on the basis of $> 1'$ resolution IRAS far-infrared colors coupled with a lack of bright centimeter wavelength emission (Molinari *et al.* 1996; Sridharan *et al.* 2002). However, detailed studies of individual MYSOs from these samples have consistently shown that they contain not a single protostar but a cluster (Hunter *et al.* 2006; Cyganowski *et al.* 2007, 2011; Brogan *et al.* 2008). Furthermore, members of a single cluster can exhibit a wide range of massive star formation signposts (e.g., Brogan *et al.* 2009; Hunter *et al.* 2008), suggesting a range of mass and/or evolutionary states. Thus the term MYSO is really synonomous with massive proto-cluster as opposed to the previous concept of a single massive protostar.

A wide variety of signposts for MYSOs have been established: H_2O and CH_3OH masers, ultracompact (UCHII) and hypercompact (HCHII) regions, dense dust cores, warm (> 30 K) NH_3 cores, massive outflows, hot core line emission, and infrared dark clouds (IRDCs). Several as yet unproven but plausible evolutionary sequences amongst these signposts have been proposed (e.g., Churchwell 2002). For masers in particular, Class I and II CH_3OH masers are thought to be early-stage, H_2O intermediate-stage, and OH late-stage tracers (e.g., Ellingsen *et al.* 2007). However, for the most part, this zoo of

phenomena has been compiled from a heterogeneous set of observations with varying angular resolution, and by and large ignores the likely clustered nature of the observed star formation. Thus, subsequent correlation analyses are plagued by sensitivity and angular resolution mismatches, astrometric uncertainties or time variability. To advance this field of study, simultaneous high angular resolution observations of a majority of these diagnostic signposts are essential, and must be performed at wavelengths long enough to penetrate the high column densities of dust and with a high enough angular resolution to distinguish individual massive protostars.

Under the auspices of the NRAO Resident Shared Risk Program (RSRO), we have carried out a K-band ($\sim$ 24 GHz) study of 22 MYSOs in 1.3 cm continuum and a comprehensive set of diagnostic lines. This survey is unique in that it samples a wide range of massive star formation signposts *simultaneously* for the first time. Ultimately our goal is to identify possible observational discriminators of evolutionary state, and answer the questions: (1) Is there a correlation between gas temperature and mid-IR luminosity? (2) Is there a correlation between gas temperature, density, or compactness and presence of hot core line emission? (3) When do hot cores develop – is detectable free-free emission required? (4) Does the level of source multiplicity correlate with other diagnostics like temperature, and density? To answer these questions we assembled and observed an NH_3-selected sample of 22 MYSOs as described below.

2. The Observed Sample

Cyganowski *et al.* (2008) compiled a promising new catalog of MYSO candidates ($\sim$ 300), based on the presence of extended 4.5 μm emission in the *Spitzer* GLIMPSE Legacy Survey – emission that is thought to arise predominantly from shocked H_2 lines (from outflows) within the 4.5 μm continuum bandpass. About half of the cataloged EGOs reside in IRDCs – thought to be the birth sites of massive stars (e.g., Rathborne *et al.* 2006). More recently, Cyganowski *et al.* (2009) have confirmed that these sources do contain massive, actively accreting protostars from VLA observations of 20 EGOs in 6.7 GHz Class II CH_3OH masers (signpost of MYSOs) and 44 GHz Class I CH_3OH masers (signpost of outflows), and single dish detections of thermal CH_3OH, $H^{13}CO^+$, and SiO. About 2/3 of the cataloged EGOs in the northern sky have also been observed in NH_3 (1,1) to (3,3) using the Nobeyama 45-m with a 94% detection rate (66 sources, 65″ resolution; Cyganowski *et al.*, in prep, also see proceedings in this volume). From the NH_3 observed EGO subsample, we selected 20 of the strongest [$T_A(NH_3\ (1,1)) > 0.7$ K; all detected in NH_3 (1,1) to (3,3)] to include in the current survey (14 of these overlap with the Cyganowski *et al.* (2009) VLA EGO subsample). We also include 2 IRDCs that are not EGOs, but are otherwise similar, and were observed previously by the VLA in NH_3 (1,1) and (2,2) (Devine *et al.* (2011) and show saturated NH_3 rotation temperatures and outflows. Most prior MYSO samples have been selected based on having at most weak free-free emission, in order to concentrate on (presumably) younger regions (e.g., Molinari *et al.* (1996); Sridharan *et al.* (2002). To avoid this potential bias, and provide a contrasting sample for the (presumably) younger EGO/IRDC sources, 9 of the objects are known to harbor UCHII or weak HCHII/wind counterparts. All 22 MYSOs in the sample also have 1.2 mm counterparts in the CSO BOLOCAM Galactic Plane Survey (Rosolowsky *et al.* 2010).

Salient facts about the sample sources are summarized in Table 1, with the sources separated into two distance categories: 2–4 kpc and 4–6 kpc. The distances have been consistently derived from the NH_3 LSR velocities using the new Galactic rotation curve of Reid *et al.* (2009); we assume the sources lie at the near distance. This assumption is

https://doi.org/10.1017/S1743921312007594 Published online by Cambridge University Press

almost certainly valid for the IRDC sources (18/22) since they are observed in silhouette against the Galactic background. Thus, we have created a sample that is unified by the presence of dense gas, dust, and outflows and lie at distances between 2–6 kpc. In contrast, the sample exhibits a wide range of mid-IR morphology, 24 μm derived luminosity, as well as a range in free-free ionized continuum properties. In addition to the targeted sources, we may also make a number of serendipitous detections from other mid-IR bright sources in the 2′ diameter FWHP primary beam. Massive star forming cores have typical sizes of 0.1 pc, and at a distance of 2 kpc (6 kpc), 4″ (1.3″) is equal to a physical scale of 0.04 pc or 8,000 AU. This is the physical scale that is essential to probe with this survey, so we observed the 2–4 kpc sample in the D (or DnC) configuration from September to December 2010 and the the 4–6 kpc sample in the C-configuration (or CnB) configuration from January to April 2011.

Table 1. The Observed Sample

Source	D kpc	H_2O maser	Methanol Masers 6.7 GHz	44 GHz	EGO	IRDC	Ionized gas	Methanol 25 GHz maser	Ammonia (3,3) maser
D-configuration sources (D = 2–4 kpc)									
G10.29−0.13	2.2	Y	Y	Y	Y^V	Y		Y	N
G10.34−0.14	2.1	Y	Y	Y	Y^V	Y		Y	Y
G11.92−0.61	3.8	Y	Y	Y	Y^V	Y	Weak	Y	Y
G14.33−0.64	2.8	Y	Y	Y	Y	Y		Y	Y
G14.63−0.58	2.3	Y	–	–	Y	Y		N	N
G19.36−0.03	2.4	Y	Y	Y	Y^V	Y		Y	Y
G22.04+0.22	3.6	Y	Y	Y	Y^V	Y		Y	N
G24.92−0.16	3.3	N	–	–	N	Y		N	Y
G24.94+0.07	3.0	N	Y	Y	Y^V	N	Weak	N	Y
G28.28−0.36	3.3	N	Y	N	Y^V	N	Weak	N	N
G35.03+0.35	3.4	Y	Y	Y	Y^V	Y	UCHII	Y	Y
DNC-configuration sources (D = 2–4 kpc)									
G12.42+0.50	2.6	Y	–	–	Y	Y	UCHII		
C-configuration sources (D = 4–6 kpc)									
G12.91−0.03	4.4	Y	–	–	Y	Y			
G16.59−0.05	4.2	Y	Y	Y	Y	Y			
G18.67+0.03	4.9	N	Y	Y	Y^V	N			
G18.89−0.47	4.5	Y	Y	Y	Y^V	Y			
G25.27−0.43	4.0	N	Y	Y	Y^V	Y			
G28.83−0.25	5.0	N	Y	Y	Y^V	Y	Weak		
G45.47+0.05	4.8	Y	Y	Y	Y	Y	UCHII		
G49.27−0.34	5.6	Y	N	Y	Y^V	Y	UCHII		
CNB-configuration sources (D = 4–6 kpc)									
G08.67−0.35	4.5	Y	Y	Y	N	Y	UCHII		
G12.68−0.18	4.7	Y	Y	–	Y	N			

EGO column: Y=EGO from Cyganowski *et al.* (2008) catalog, Y^V = EGO also in Cyganowski *et al.* (2009) VLA CH_3OH maser survey sample.
Ionized column: Weak means < 1 mJy beam^{-1} at 3.6cm in the Cyganowski *et al.* (2011) continuum survey

https://doi.org/10.1017/S1743921312007594 Published online by Cambridge University Press

3. Key Diagnostics

To sample a wide range of potential diagnostics of MYSO evolutionary state and answer the questions posed above, we have used the WIDAR correlator with sixteen 8 MHz subbands to simultaneously observe the key diagnostics described below at a spectral resolution of ~ 0.4 km s^{-1}. The correlator setup is shown in Figure 1.

Ammonia: The NH_3 ladder from (1,1) to (6,6) with E_l=23–400 K allows us to fit for the rotation temperature (T_R) of the hot dense gas, as well as NH_3 column density, and core diameter. In the past, only the (1,1) and (2,2) transitions were typically observed, which saturate for $T_R > 25$ K. Indeed, a recent VLA study of several IRDCs in NH_3 (1,1) and (2,2) has demonstrated that toward dense NH_3 cores with mid-IR counterparts, T_R is too high to be constrained by the two lowest transitions alone (Devine *et al.* 2011). For sources in confused regions, the (1,1) line can be difficult to image, but the emission in (2,2) and higher is generally very compact.

Hot Core Lines: Thermal emission from the CH_3OH-E ladder from E_l=35 - 150 K can provide an independent check on T_R (e.g. Menten *et al.* 1986), and establish whether the source harbors "hot core" line emission. Comparing the NH_3 and CH_3OH T_R is interesting because CH_3OH is often used to calculate hot core temperatures in the (sub)millimeter band (Brogan *et al.* 2007, 2009). Several of the lower lying transitions have been observed as Class I masers (e.g. Menten *et al.* 1986).

Continuum Emission: For sources with jets, HCHII, or UCHII regions, we have obtained images of the free-free emission with resolution matching the molecular gas. For sources lacking either an HII region designation or Y$^{\rm V}$ EGO designation in Table 1, these are the first sensitive high resolution cm-λ observations.

Radio Recombination Lines: H63α and H64α also lie within our bandpass, and when combined with free-free continuum, these RRLs can be used to measure the density, electron temperature, and mass of the ionized gas.

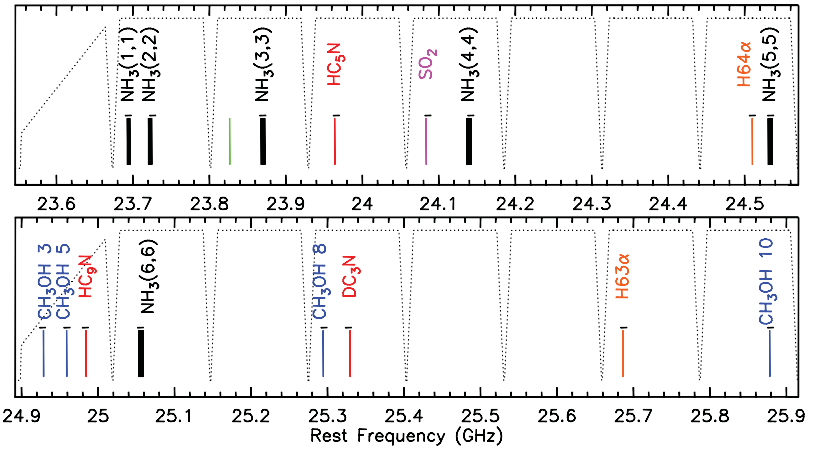

Figure 1. Sample JVLA correlator setup showing the sixteen 8 MHz spectral windows superposed on the inherent filter shape (dotted line).

4. Results

Processing of the D-configuration (2–4 kpc) sample has been completed, and the images reveal complexity in terms of core multiplicity, gas temperatures and kinematics, shocks, masers, and continuum properties. The results on the first source, G35.03+0.35, appeared in Brogan *et al.* (2011) and are summarized in Fig. 2. We detect compact

https://doi.org/10.1017/S1743921312007594 Published online by Cambridge University Press

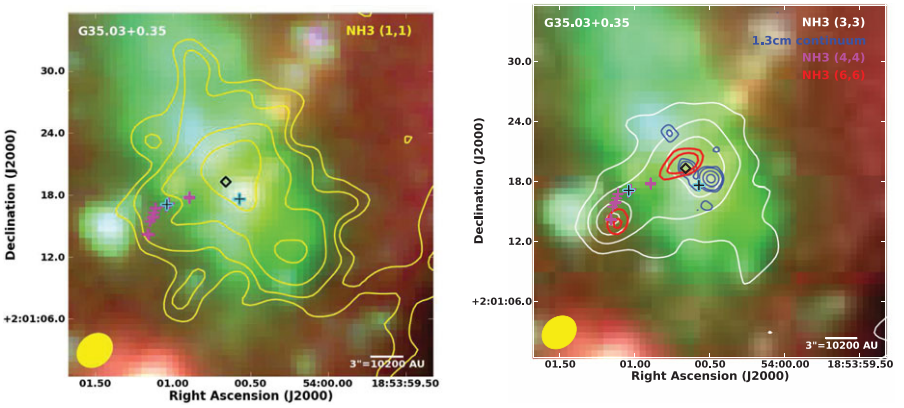

Figure 2. *Spitzer* GLIMPSE 3-color image with RGB= 8, 4.5, and 3.6 μm. Left: NH_3 (1,1) emission in yellow contours. Right: NH_3 (3,3) emission in white contours (most extended), NH_3 (6,6) in red, and 1.3 cm continuum in blue. The synthesized beam is shown in the lower left. Also see Brogan *et al.* (2011)

NH_3 cores in all of the fields, some seen in (1,1) and (2,2) only, and others up through NH_3 (6,6) - indicating the presence of "hot cores". 25 GHz CH_3OH maser emission is present in 7 out of 11 sources in close proximity in position and velocity to 44 GHz masers. Weak thermal emission in CH_3OH is also detected in some sources. We also detect non-thermal emission in the NH_3 (3,3) transition in 7 out of 11 sources, excited by outflow shocks (e.g. Zhang *et al.* 1999). Our preliminary results already demonstrate the powerful new capability offered by the WIDAR correlator and the JVLA. Additionally, millimeter follow-up observations have been obtained for more than half the sample with the remaining sources hopefully observed soon. When analysis of the survey is complete we expect to have a much greater understanding of the physical properties, and multiplicity of massive forming proto-clusters.

References

Brogan, C. L., Hunter, T. R., Cyganowski, C. J., Friesen, R., *et al.* 2011, *ApJL*
Brogan, C. L., Hunter, T. R., Cyganowski, C. J., Indebetouw, R., *et al.* 2009, *ApJ*, 707, 1
Brogan, C. L., Hunter, T. R., Indebetouw, R., *et al.* 2008, *Ap&SS*, 313, 53
Brogan, C. L., Chandler, C. J., Hunter, T. R., *et al.* 2007, *ApJ*, 660, L133
Churchwell, E. 2002, *ARAA*, 40, 27
Cyganowski, C. J., Brogan, C. L., & Hunter, T. R. 2011, *ApJ*, 743, 56
Cyganowski, C. J., Brogan, C. L., Hunter, T. R., & Churchwell, E. 2009, *ApJ*, 702, 1615
Cyganowski, C. J., *et al.* 2008, *AJ*, 136, 2391
Cyganowski, C. J., Brogan, C. L., & Hunter, T. R. 2007, *AJ*, 134, 346
Devine, K., Chandler, C. J., Brogan, C. L., *et al.* 2011, *ApJ*, 733, 44
Ellingsen, S. P. *et al.* 2007, *IAU Symposium*, 242, 213
Hunter, T. R., Brogan, C. L., Indebetouw, R., & Cyganowski, C. J. 2008, *ApJ*, 680, 1271
Hunter, T. R., Brogan, C. L., Megeath, S., *et al.* 2006, *ApJ*, 649, 888
Menten, K. M., Walmsley, C. M., Henkel, C., & Wilson, T. L. 1986, *A&A*, 157, 318
Molinari, S., Brand, J., Cesaroni, R., & Palla, F. 1996, *A&A*, 308, 573
Reid, M. J., *et al.* 2009, *ApJ*, 700, 137
Rathborne, J. M., Jackson, J. M., & Simon, R. 2006, *ApJ*, 641, 389
Rosolowsky, E., Dunham, M. K., Ginsburg, A., *et al.* 2010, *ApJS*, 188, 123
Sridharan, T. K., Beuther, H., Schilke, P., Menten, K. M., & Wyrowski, F. 2002, *ApJ*, 566, 931
Zhang, Q., Hunter, T. R., Sridharan, T. K., & Cesaroni, R. 1999, *ApJ*, 527, L117
Zinnecker, H. & Yorke, H. W. 2007, *ARAA*, 45, 481

https://doi.org/10.1017/S1743921312007594 Published online by Cambridge University Press